Characterization of Immune Cell Infiltration and Collagen Type III Disorganization in Human Secondary Lymphedema: A Case-control Study

Andreas Spörlein*†
Christoph Hirche, MD*‡
Juan Enrique Berner, MD, MSc, FRCS§¶
Ulrich Kneser, MD*
Patrick A. Will, MD, MSc*‖

Background: Secondary lymphedema (SL) affects 120 million people globally, posing a lifelong burden for up to 37% of cancer survivors. Chronic inflammation and progressive fibrosis are key drivers of SL, yet detailed characterization of immune cell subpopulations across lymphedema stages is lacking. This study aimed to investigate the immunologic profile of lymphedematous skin and its association with extracellular matrix changes, which could serve as clinical biomarkers or therapeutic targets.

Methods: This case-control study analyzed the skin from 36 patients with and without SL, using immunofluorescence to quantify T cells, B cells, macrophages, and their subpopulations. Collagen quantity and composition were examined using picrosirius red staining, and mast cell infiltration was assessed with toluidine blue staining. Early and late SL stages were compared to identify histomorphological and immunologic correlates of stage progression.

Results: We found a predominance of CD4+ T cells and mast cells in SL skin (1.4/mm² versus 1.0/mm², $P < 0.01$; 1.2/mm² versus 0.2/mm², $P < 0.0001$) and a higher ratio of collagen III to collagen I fibers (51.6% versus 75.0%, $P < 0.001$). M2 macrophages were more abundant in late-stage than in early-stage lymphedema (1.7/mm² versus 1.0/mm², $P = 0.02$).

Conclusions: This study demonstrated a shift toward CD4+ T cell and mast cell infiltration in SL skin, correlating with extracellular matrix disorganization and an altered collagen III/I ratio. These findings enhance our understanding of the cellular and morphological changes in SL, potentially guiding future diagnostic and therapeutic strategies. *(Plast Reconstr Surg Glob Open 2024; 12:e5906; doi: 10.1097/GOX.0000000000005906; Published online 17 June 2024.)*

INTRODUCTION

Secondary lymphedema (SL) affects 120 million patients worldwide and is associated with chronic swelling, functional impairment, recurrent infections, reduced quality of life, and substantial economic burden.[1–3] It is often the result of cancer treatments,[4] most often breast cancer, but may also arise after trauma in up to 37% of cases.[5] Due to advances in the field of oncology, wider access to treatment, and better survival rates, the prevalence and burden of SL will likely increase in the future.[6]

Not all patients who undergo extensive lymphatic dissection and drainage disruption develop SL.[7] A recent prospective cohort study showed that the risk of SL clinical onset peaks between 12 and 30 months after surgery,

Disclosure statements are at the end of this article, following the correspondence information.

Related Digital Media are available in the full-text version of the article on www.PRSGlobalOpen.com.

yet the clinical detection of SL is highly variable.[7,8] Not all patients will show a linear progression through stages of the disease, from subclinical condition without swelling (stage 0); accumulation of protein-rich fluid with intermittent pitting edema reversible by extremity elevation (stage I); persistent swelling, onset of fibrosis, and fat accumulation (stage II); to lymphostatic elephantiasis with local skin changes (stage III).[9] Although retrospective case-control analyses have identified several risk factors, including lymph node resection, radio- and chemotherapy, obesity, and infection,[4] no definitive correlation has been proven between these risk factors and SL clinical progression, according to a recent meta-analysis.[10]

It has been suggested that protein accumulation and lymphatic stasis are triggers for inflammation.[11,12] The role of T cells and the Th2 response in the development of lymphedema have been described in both basic research and clinical studies.[12–14] An association was found between specific lymphedema symptoms and transforming growth factor β, interleukin-4, -6, -13, and tumor necrosis factor α (TNFα).[15] These cytokines are largely involved in pro-inflammatory, profibrotic, and proadipogenic processes.[16] Furthermore, these cytokines were found to be negative regulators of lymphangiogenesis, proliferation of lymphatic endothelial cells, and tube formation in vitro.[17] These findings suggest a complex interplay between chronic inflammation, fibrosis, and failure of lymphatic regeneration.[18,19] At the clinical level, the treatment of cell-mediated inflammation in SL seems promising.[20] The continuous use of nonsteroidal antiinflammatory drugs has been found to reverse experimental SL in a mouse tail model[21] and reduce skin thickness and histopathologic abnormalities in both an open-label and placebo-controlled clinical trial.[22]

SL preclinical models provide important mechanistic insights, such as in preventing SL development through neutralizing CD4+ cells with antibodies or applying topical tacrolimus immunosuppression following SL induction.[23,24] There is still a gap in the characterization of tissue changes and immune cell subpopulations across stages in human SL and there are no viable cellular biomarkers or targets.[23,24]

As a hypothesis for this study, we suggest that tissue infiltration of immune cell populations (including CD4+ and CD8 + T cells, B cells, M1 and M2 polarized macrophage subtypes, and mast cells) is increased in human SL compared with that in healthy control tissue. Additionally, we hypothesize that there are differences in cell infiltration between early and late-stage SL, related to morphological changes in the quantity and quality of collagen.

MATERIALS AND METHODS

Sample Collection and Processing

This observational case-control study received ethics committee approval in the state of Rheinland-Pfalz (approval no.: 2020 15173). Full-thickness skin tissue samples from patients with SL undergoing lymphatic

---

Takeaways

Question: The study addresses the characterization of immune cell infiltration and collagen type III disorganization in secondary lymphedema (SL) skin, aiming to identify potential clinical biomarkers or therapeutic targets.

Findings: Using immunofluorescence and histological staining, the study found a dominant infiltration of CD4+ T cells and mast cells in SL, alongside a higher ratio of collagen III to I, indicating immune cell shift and extracellular matrix disorganization. M2 macrophages were notably more abundant in late-stage SL.

Meaning: This study highlights the immune and morphological shifts in SL, advancing our understanding of its cellular underpinnings and aiding early lymphedema diagnosis and stage determination.

microsurgery, either lymphovenous anastomosis or lymph node transfer, were collected after obtaining consent. Patients were classified as early-stage SL if equivalent to stages 1 and 2 according to the International Society of Lymphology, or as late-stage SL if equivalent to International Society of Lymphology stage III.[9] All patients had previously been treated conservatively for at least 6 months, including compression garments and manual lymphatic drainage. Patients with acute or chronic infections, such as patients with elevated leukocyte count or C-reactive protein levels, were excluded. SL samples from the upper extremity were collected from the distal forearm, and lower limb samples were harvested from the distal leg, close to the lateral malleolus. As the control group, healthy skin tissue from the free flap donor site during reconstructive surgery was used. The sample sizes were 14 and 22 in the lymphedema and control groups, respectively. An overview of the inclusion and exclusion criteria is presented in the Supplemental Digital Content 1. (**See figure, Supplemental Digital Content 1,** which displays inclusion and exclusion criteria for the observational case-control study. **http://links.lww.com/PRSGO/D292**)

The tissue specimens were fixed in paraformaldehyde, dehydrated in an alcohol sequence, cleared in xylene, paraffinized, cut into slices of 5-µm thickness, and transferred to electrostatic fixation slides. Before histomorphological staining and immunofluorescence, the tissue was deparaffinized in xylene and rehydrated.

Histomorphological Staining

Hematoxylin and eosin staining was performed for morphological overview.[25] Nuclear staining in Mayer hemalum solution was followed by differentiation with an HCl/ethanol solution and bluing in ammonia water. Counterstain was performed in aqueous eosin Y-solution. Picrosirius red (PSR) staining was used for collagen analysis.[26–29] The slides were stained with Weigert iron hematoxylin, washed with flowing tap water, stained with PSR staining solution consisting of direct red 80 and saturated picric acid, and then dipped in an acetic acid solution. Toluidine blue staining allows for the detection and

quantification of mast cell infiltration.[30] The sections were stained in a solution consisting of TB O dissolved in ethanol and acidified sodium chloride at a pH of 2.0. After staining, the slides were rehydrated, cleared with xylene again, and mounted on coverslips.

Immunofluorescence

Tissue antigens were demasked using the IHC-Tek Epitope Retrieval Steamer (IHC World, Ellicott City, Md.). To reduce nonspecific binding, 5% donkey serum was added to phosphate-buffered saline. A standardized protocol was followed for immunophenotyping[31]: primary antibodies were appropriately diluted in 1% normal serum in phosphate-buffered saline and incubated at 4°C in a humid chamber for 20h: anti-CD3 (sc-20047, 1:100), anti-CD4 (sc-19641, 1:100), anti-CD8 (sc-1177, 1:100), anti-CD68 (sc-20060, 1:100), anti-CD163 (sc-20066, 1:100), anti-NOS2 (sc-7271, 1:100), from Santa Cruz Biotechnology, Dallas, Tex., and anti-CD20 (CSB-MA000204, 1:200) from Cusabio, Houston, Tex. Alexa Fluor 488 conjugated donkey antimouse and donkey antigoat secondary antibodies, depending on the primary antibody host species, were incubated at room temperature in a humid chamber for 60 minutes (715-545-150 and 705-545-147, Jackson ImmunoResearch, West Grove, Pa.). An antifade mounting medium with the nuclear stain DAPI (Vector Laboratories, Newark, Calif.) was used for coverslipping.

Microscopic Analysis

High-magnification whole-slide microscopic images were obtained. All investigators were blinded to the sample origin. A circularly polarized light filter was used to acquire PSR images. Color thresholding in Fiji[32] was used for quantification of the total collagen area of PSR. Although thick collagen fibers mainly consisting of type I collagen show a red hue in circularly polarized light, thin collagen fibers mainly consisting of type III collagen show a green-yellow hue.[33,34]

Statistical Analysis

Statistical analysis was performed using GraphPad Prism (version 9.4.0). SL patients were compared with the control group, and a subgroup analysis distinguishing early- and late-stage SL was performed. The unpaired *t* test was used for parametric data and the Mann-Whitney test for nonparametric data as determined by the Shapiro Wilk test with an alpha level of 0.05. The cutoff for statistical significance was a *P* value less than 0.05. The sample size calculation was performed using G-power (version 3.1). The inputs were a power of 80% (0.8), two-tailored, size effect 0.8, alpha error 0.05, and allocation ratio 1.

Primary and Secondary Endpoints

The primary endpoint of this study was a significant increase in lymphocyte subpopulations in lymphedema skin tissue. The secondary endpoints were to detect increased infiltration of other immune cells and relate this presence to a compositional change in collagen I or III in early- or late-stage SL.

RESULTS

The lymphedema patients had a mean age of 54.3 ± 16.1 years, a mean body mass index (BMI) of 28.0 ± 8.6 kg per m², and nine (64.3%) were women. Ten patients had lower extremity SL, whereas four presented upper extremity SL. Ten patients had early-stage SL, and four had late-stage SL. Four patients had post-traumatic SL, whereas 10 patients had SL induced by cancer treatment. The primary cancer type was breast cancer in three patients, urologic or gynecologic cancer in three, melanoma in two, sarcoma in one, and lymphoma in one.

In the control group, 18 patients (72.7%) were men, mean age was 64.9 ± 18.1 years, and mean BMI was 29.9 ± 5.8 kg per m². Control skin was obtained from the back of 16 patients who underwent a latissimus dorsi flap, from the abdomen of three patients who had a DIEP flap, and from the thigh of three patients receiving a myocutaneous gracilis flap. An epidemiological data summary is provided in Supplemental Digital Content 2. (**See figure, Supplemental Digital Content 2,** which displays the baseline characteristics of the lymphedema and control groups. **http://links.lww.com/PRSGO/D293**.)

The SL group presented a higher proportion of female patients (64.3 versus 27.2%, *P* = 0.04). Differences in age (54.3 ± 16.1 versus 64.9 ± 18.1 years, *P* = 0.08) and BMI (28.0 ± 8.6 versus 29.9 ± 5.8 kg/m², *P* = 0.42) were statistically nonsignificant. An overview of all statistical tests and results is provided in Supplemental Digital Content 3. (**See figure, Supplemental Digital Content 3,** which displays the overview of the main results including statistical test and significance. **http://links.lww.com/PRSGO/D294**.)

Lymphedema Skin Has More Collagen III Than Collagen I Fibers Compared with Control Skin

PSR revealed that the fraction of tissue area that was covered by collagen was lower in the SL group than in the control group ($45.4 \pm 10.0\%$ versus $63.5 \pm 7.2\%$, *P* < 0.0001). Regarding the collagen composition for SL stages, no difference was observed between early- and late-stage ($45.6 \pm 9.6\%$ versus $45.0 \pm 13.8\%$, *P* = 0.93; Figs. 1 and 2) (**See figure, Supplemental Digital Content 4,** which displays collagen as a fraction of total dermal area determined by picrosirius red staining: box plot with mean, interquartile range, and whiskers from minimum to maximum. **http://links.lww.com/PRSGO/D295**.) (**See figure**, **Supplemental Digital Content 5,** which displays a fraction of thick and thin collagen fibers determined by picrosirius red staining: box plot with mean, interquartile range, and whiskers from minimum to maximum. **http://links.lww.com/PRSGO/D296**.). Thick collagen fibers, which seem red under circularly polarized light and correlate with collagen I, were significantly less prevalent in lymphedematous tissues than in healthy skin (51.6% (IQR: 40.3–60.4%) versus 75.0% (IQR: 60.6–79.6%), *P* < 0.001). Despite observing notably more thick collagen fibers in early-stage SL than in late-stage of SL during microscopic analysis, the difference proved to be statistically nonsignificant ($48.8 \pm 11.8\%$ versus $59.3 \pm 7.2\%$,
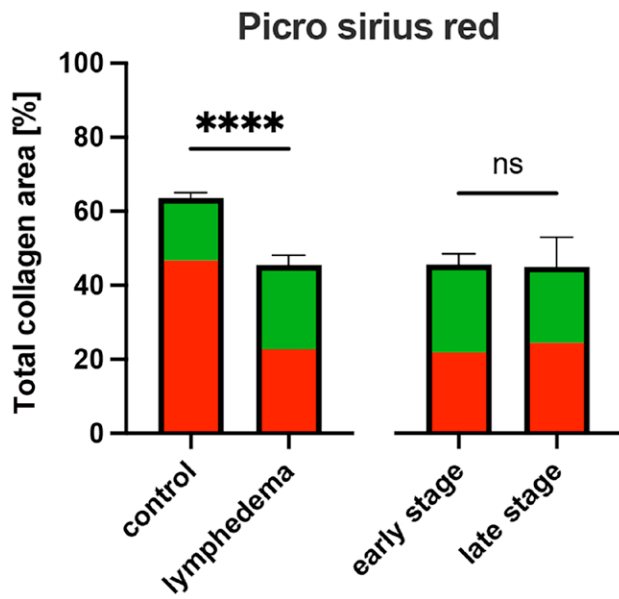
Picro sirius red

Fig. 1. Collagen as a fraction of total dermal area determined by picrosirius red staining: mean with standard error of the mean. Additionally, the fraction of thick and thin collagen fibers is shown in red and green, respectively. ****$p < 0.0001$.

$P = 0.18$). Although thin collagen fibers, appearing yellow-green and correlating to collagen III, were significantly more prevalent in SL than in control tissue (48.4% (IQR: 39.6–59.7%) versus 25.9% (IQR: 20.4–39.4), $P < 0.001$), the perceived increase in collagen III in the early-stage was nonsignificant compared with late-stage SL (51.2 ± 11.8% versus 40.7 ± 7.2%, $P = 0.18$).

Lymphedema Skin Showed an Immune Cell Subpopulation Shift toward Mast Cells and T Helper Lymphocytes

TB revealed a significantly increased infiltration of mast cells in SL compared with healthy skin (1.2/mm² (IQR: 0.6–1.7/mm²) versus 0.2/mm² (IQR: 0.1–0.4/mm²), $P < 0.0001$). A higher infiltration of mast cells was noticed in early-stage compared with late-stage SL yet failed to reach statistical significance (1.1 ± 0.8/mm² versus 0.6 ± 0.3/mm², $P = 0.28$; Figs. 3 and 4). Mast cells in lymphedematous tissue appeared more clustered than those in the control tissue, and most were found in the superficial part of the dermal layer.

Immunofluorescence imaging (Fig. 5) revealed a highly increased cell infiltration in SL in comparison to healthy skin for CD3, a pan T-cell marker (2.9 ± 1.0/mm² versus 1.9 ± 0.85/mm², $P < 0.01$). [**See figure, Supplemental Digital Content 6,** which displays immunofluorescence imaging of CD3: whole-slide bright-field images and representative regions of interest in 20× magnification of human SL (A–C) and healthy control tissue (D–F) are shown. The mouse anti-CD3 primary antibody was labeled in green by an Alexa Fluor 488 conjugated donkey antimouse secondary antibody. Scale bar = 100 µm. **http://links.lww.com/PRSGO/D297**.]

Most of these T cells were CD4 positive [1.4/mm² (IQR: 1.0–2.5/mm²) versus 1.0/mm² (IQR: 0.6–1.4/mm²); $P < 0.01$]. [**See figure, Supplemental Digital Content 7,** which displays immunofluorescence imaging of CD4: whole-slide bright-field images and representative regions of interest in 20× magnification of human SL (A–C) and healthy control tissue (D–F) are shown. The mouse anti-CD4 primary antibody was labeled in green by an Alexa Fluor 488 conjugated donkey antimouse secondary
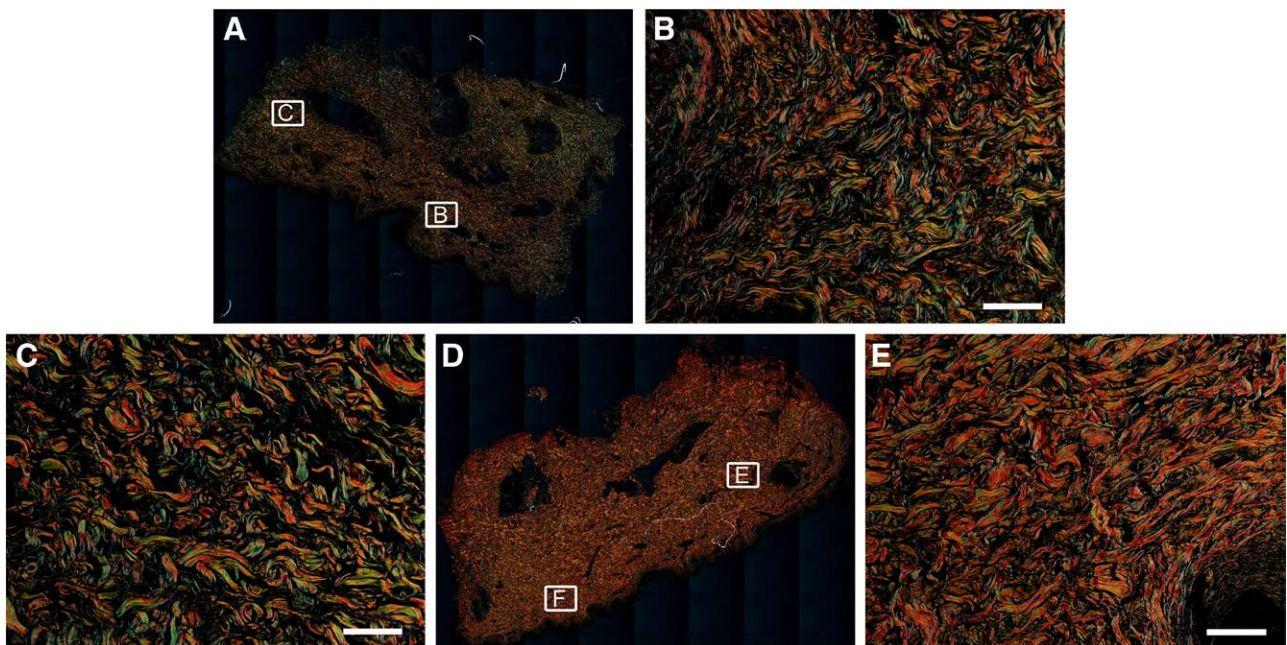

Fig. 2. Collagen analysis with picrosirius red staining. Whole-slide images and representative fields of view in 20× magnification of SL (A–C) and healthy control tissue (D–F) are shown respectively. Scale bar = 100 µm.
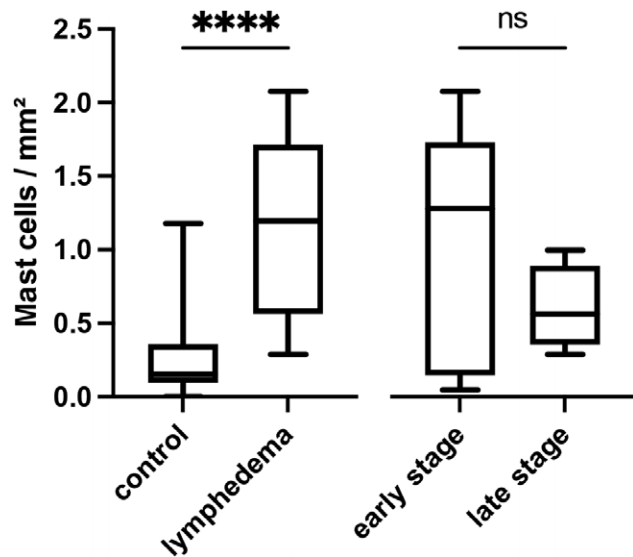
Fig. 3. Number of mast cells per mm² determined by TB staining: Box plot with mean, interquartile range, and whiskers from minimum to maximum. ****$p < 0.0001$.

antibody. Scale bar = 100 μm. **http://links.lww.com/ PRSGO/D298.**] No differences were detected for CD8, a marker for cytotoxic T cells ($1.5 \pm 0.6/mm^2$ versus $1.4 \pm 0.8/mm^2$, $P = 0.66$), or CD20, a pan B-cell marker [$1.4/mm^2$ (IQR: 1.0–$2.2/mm^2$) versus $1.4/mm^2$ (IQR: 0.8–$2.5/mm^2$), $P = 0.60$]. More cells positive for the pan macrophage marker[35] CD68 were observed in lymphedematous tissue; however, this difference was not statistically significant ($2.4 \pm 1.2/mm^2$ versus $2.2 \pm 1.2/mm^2$,

$P = 0.57$). A further subanalysis of CD163 and iNOS positive M2 and M1 polarized macrophage[36,37] revealed no differences between lymphedematous and control skin samples [$1.2 \pm 0.5/mm^2$ versus $1.1 \pm 0.5/mm^2$, $P = 0.64$ and $1.0/mm^2$ (IQR: 0.7–$2.0/mm^2$) versus $1.5/mm^2$ (IQR: 0.8-$2.1/mm^2$), $P = 0.67$].

M2 Macrophages Are More Abundant in Late Lymphedema Stages

The immunofluorescence subgroup analysis comparing early- and late-stage SL (Fig. 6) showed an increased presence of CD163+ cells or M2 polarized macrophages in late-stage SL ($1.0 \pm 0.4/mm^2$ versus $1.7 \pm 0.4/mm^2$, $P = 0.018$; Fig. 6). [**See figure, Supplemental Digital Content 8,** which shows immunofluorescence image of CD163, which displays whole-slide bright-field images and representative fields of view in 20× magnification of human SL in the early-stage (A–C) and late-stage group (D–F). The mouse anti-CD163 primary antibody was labeled in green by an Alexa Fluor 488 conjugated donkey antimouse secondary antibody, indicating M2 polarized macrophages. Scale bar = 100 μm. **http:// links.lww.com/PRSGO/D299.**] All other markers did not reveal relevant quantitative differences between early- and late-stage SL.

DISCUSSION

This study revealed a distinct difference in macrophage polarization in SL. We observed an increase in M2 polarized macrophages in late-stage SL (CD163+). M1 polarized macrophages are attributed to acute inflammation and the host response to pathogens, whereas M2
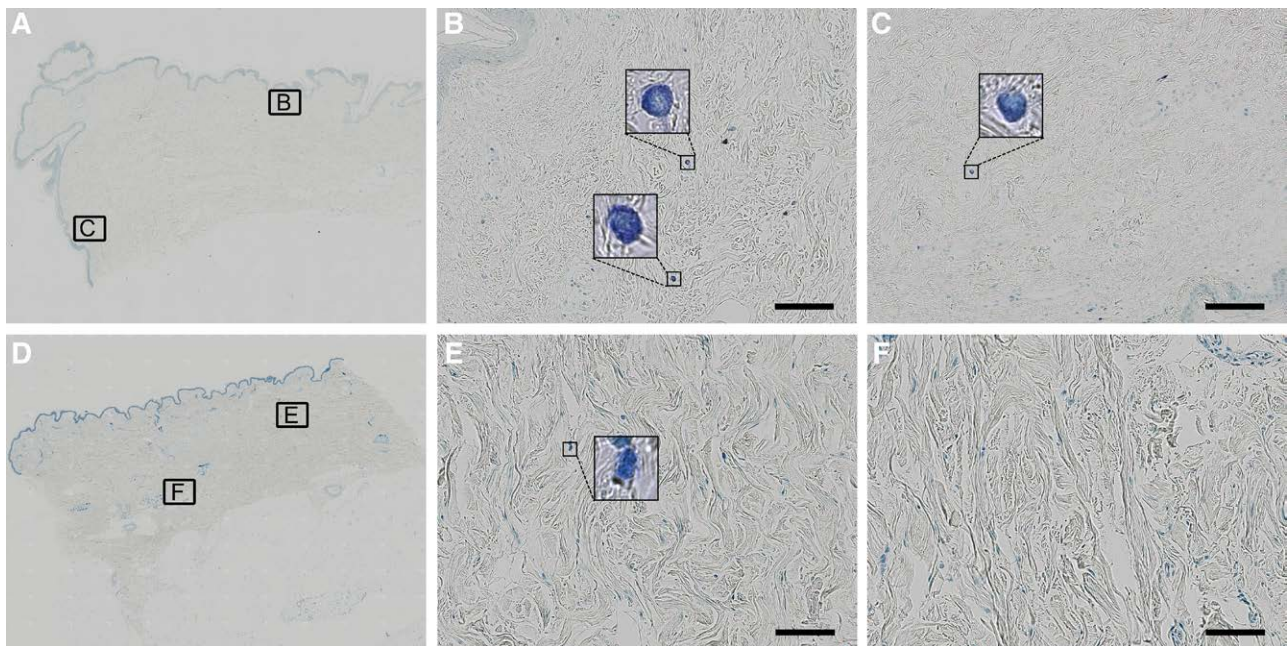

Fig. 4. Mast cell identification with TB staining. Whole-slide images and representative viewing fields in 20× magnification of SL (A–C) and healthy control tissue (D–F) are displayed. The mast cells are visualized in dark blue to purple, and their typical granules become visible under higher magnification. Scale bar = 100 μm.
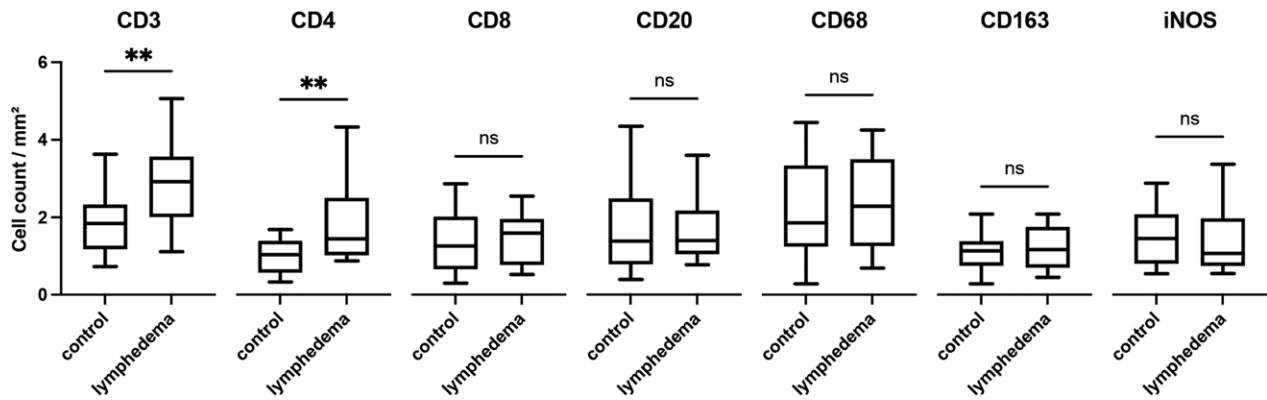
Fig. 5. Immunofluorescence imaging comparing human SL and healthy control tissue: box plot with mean, interquartile range, and whiskers from minimum to maximum. **$p < 0.001$.
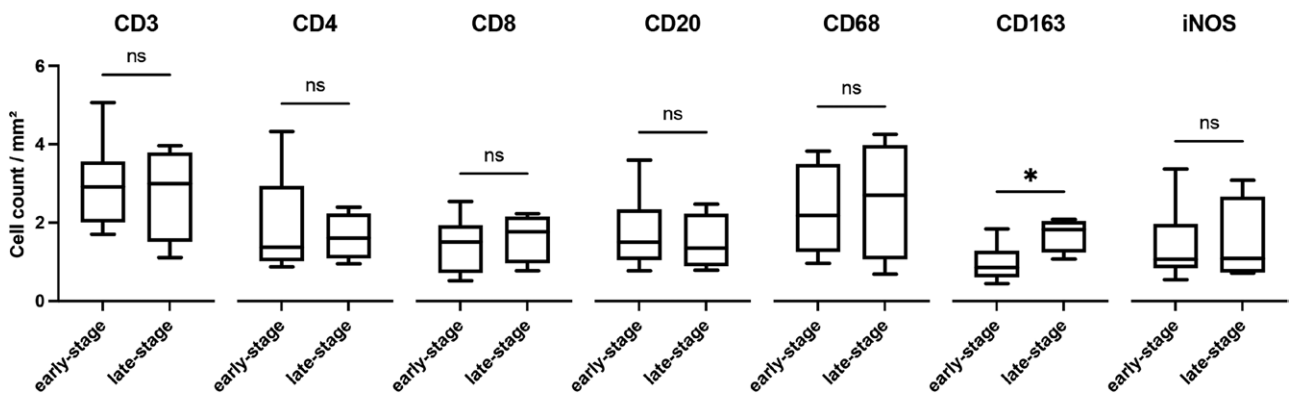

Fig. 6. Subgroup analysis for immunofluorescence imaging comparing early- and late-stage SL. Box plot with mean, interquartile range, and whiskers from minimum to maximum. *$p < 0.05$.

macrophages regulate tissue regeneration and are associated with chronic inflammation and cancer.[38,39]

A macrophage ablation model revealed that macrophage accumulation in mouse tail SL leads to impaired lymphatic function and increased fibrosis.[40] Macrophages also play an important role in lymphangiogenesis[41] and M2 polarized macrophages are key regulators of collateral lymphatic vessel regeneration.[42] Tashiro et al reported a decrease in M2 macrophages in human lymphedema adipose tissue.[43] However, little has been reported about the temporal distribution of macrophage M1/M2 subpolarization across SL stages. It has been suspected that macrophages have opposing roles in SL onset versus progression.[44] The classification of early- and late-stage SL in this study has been previously used in the literature and correlates with relevant clinical outcomes following lymphatic surgery.[45–48] The relative accumulation of M2-polarized macrophages in late-stage SL suggests that this macrophage subtype might be part of an underlying mechanism of SL progression.

We were able to validate the pathological infiltration of T cells (CD3+) and predominant presence of its T helper (CD4+) subpopulation in human lymphedema skin samples, which has previously been reported in rodent tail and extremity lymphedema models.[13,49] Differences between early- and late-stages were not detected in our study despite

a previously reported positive correlation between CD4+ T cells and stage progression.[13] Interestingly, an increase in CD4+ T cells is found in SL but not in lipedema or lipohypertrophy; it is not limited to the affected limb, suggesting a systemic inflammatory response.[50,51]

An increase in toluidine-positive mast cells has been found in a knockdown mouse model of primary lymphedema, in a SL tail model, and in a smaller study of human SL.[52–54] We found a marked increase in mast cell infiltration in human SL. Mast cells liberate proinflammatory mediators, such as histamine, proteases, and derivates from the cyclooxygenase (prostaglandin) and lipoxygenase (leukotriene) pathways.[55] Such mediators facilitate vasodilation, plasma extravasation, and recruitment of T cells, granulocytes, and monocytes, which account for chronic inflammation.[55] A procoagulant effect of mast cell-derived TNF-α was shown to cause edema in a peritonitis model via fibrinous adhesions[49] and collagenesis of dermal fibroblasts via transforming growth factor β and TNFα.[56] Mast cell mediators might generate clots of fibrin and adhesions from the extravasate of lymphedema in the soft tissue, subsequently obstructing lymphatic vessels and promoting sclerotic and dysfunctional remodeling of the extracellular matrix.

Concerning the characterization of dermal collagen structure in SL,[23] we observed a higher fraction of thin

collagen fibers (mainly type III collagen) in the SL group. This is likely a manifestation of extracellular matrix disorganization,[57] consistent with a recent case-control study of eight patients with stage III SL, which reported a 54.9-fold increase in type III collagen gene transcription, and a 1.4-fold increase in type I collagen gene transcription.[58] This can be explained by fat deposition and fluid accumulation, which may lead to collagen being more spread out across the dermis. In animal models, conflicting results concerning dermal collagen density have been reported.[59] This includes a dramatic postoperative decrease in collagen density and a return to almost normal levels by day 14 in a mouse tail model of SL,[60] as well as an increase in collagen density in a Chy mouse model of primary lymphedema[61] and in a rodent hind limb model of SL.[52]

Limitations

An ideal experiment would have compared matched biopsies from lymphedematous and healthy tissues from the same patients. Excess surgical tissue was used as a control in this experiment for ethical reasons, requiring no additional trauma for any of the patients involved. Because SL is more frequent in the female population and trauma patients requiring free flaps are predominantly men, we had a higher female-to-male ratio in lymphedema patients than in the control group. We deliberately excluded all patients with chronic inflammatory comorbidities, infections of any kind, patients who had received chemotherapy or radiotherapy in the previous year, and patients taking non-steroidal anti-inflammatory drugs (NSAIDs) regularly. This rigorous exclusion was at the expense of the sample size in the case group. The study was underpowered for the detection of small differences concerning collagen quantity and type, as well as more subgroup analyses such as a comparison between the immune cell subpopulations of the lower and upper extremities. Studies have suspected gender differences in lymphedema because of a possible influence of sex hormones[62]; nonetheless, we did not detect any differences, likely because of the limited sample size. The PSR staining provided evidence for a disbalance of collagen fibers in SL progression. These quantitative findings could have been confirmed by quantitative real-time PCR, in situ hybridization, and enzyme-linked immunosorbent assay/multiplex analysis.

Conclusions and Recommendations

In summary, the CD4+ T-cell-dominated inflammation during SL is correlated with distinct changes in the collagen composition. The strong accumulation of mast cells in SL is indicative of their possible contribution to fibrosis, equivalent to other chronic inflammatory diseases, as well as lymphatic vessel alteration. Our findings represent a pathophysiological translational bridge between the preclinical findings and empirical clinical evidence of NSAIDs for the treatment of lymphedema. A randomized double-blinded clinical trial showed that ketoprofen was able to reverse the edema of lymphedema and prevent fibrotic changes of the skin by inhibiting cyclooxygenase and leukotrienes of the immune cells.[62,63] A previously published SL animal model showed that ketoprofen can remodel the extracellular matrix to a more physiological constitution, indirectly preventing stage progression.[64] Future in vivo experiments of Cyclooxygenase-1 and Cyclooxygenase-2 inhibitors on mast cells, macrophages, and CD4+ depleted or knocked-out animals could be the translational next step.

Future experiments could examine immune cell subpopulations and extracellular matrix composition before and after lymphedema microsurgery. This will help determine whether restoration of the locoregional lymphatic system can prevent the progression of the inflammatory process. If an immune-cellular pattern and tissue phenotype of chronic inflammatory progression are identified, these biomarkers might guide clinicians in determining the best time point for performing specific supermicrosurgical or ablative procedures using a small biopsy.[63] Regarding capsular contracture and graft survival,[64,65] the local immunomodulatory effect of autologous stem cell transplantation as an adjuvant for supermicrosurgery should be explored in further in vivo experiments.[66]

By further understanding SL stage progression, therapies could become more personalized. Using blood small tissue samples to identify high-risk patients following lymphatic disruption could also lead to earlier and more effective treatment, even before the clinical appearance of lymphedema.[67]

Patrick A. Will, MD, MSc
Plastic Surgery Department
University Hospital Carl Gustav Carus
TU University Dresden
Fetscherstraße74, 01307 Dresden
Germany
E-mail: pwillmarks@yahoo.de

DISCLOSURE

REFERENCES

1. Taghian NR, Miller CL, Jammallo LS, et al. Lymphedema following breast cancer treatment and impact on quality of life: a review. *Crit Rev Oncol Hematol.* 2014;92:227–234.
2. Shih YC, Xu Y, Cormier JN, et al. Incidence, treatment costs, and complications of lymphedema after breast cancer among women of working age: a 2-year follow-up study. *J Clin Oncol.* 2009;27:2007–2014.
3. Warren AG, Brorson H, Borud LJ, et al. Lymphedema: a comprehensive review. *Ann Plast Surg.* 2007;59:464–472.
4. Rockson SG, Keeley V, Kilbreath S, et al. Cancer-associated secondary lymphoedema. *Nat Rev Dis Primers.* 2019;5:1–16.
5. Cormier JN, Askew RL, Mungovan KS, et al. Lymphedema beyond breast cancer: a systematic review and meta-analysis of cancer-related secondary lymphedema. *Cancer.* 2010;116:5138–5149.
6. Santucci C, Carioli G, Bertuccio P, et al. Progress in cancer mortality, incidence, and survival: a global overview. *Eur J Cancer Prev.* 2020;29:367–381.
7. McDuff SGR, Mina AI, Brunelle CL, et al. Timing of lymphedema after treatment for breast cancer: when are patients most at risk? *Int J Radiat Oncol Biol Phys.* 2019;103:62–70.
8. Yamamoto T, Matsuda N, Doi K, et al. The earliest finding of indocyanine green lymphography in asymptomatic limbs of lower extremity lymphedema patients secondary to cancer treatment. *Plast Reconstr Surg.* 2011;128:314e–321e.

9. Executive Committee of the International Society of, L. The diagnosis and treatment of peripheral lymphedema: 2020 consensus document of the International Society of Lymphology. *Lymphology*. 2020;53:3–19.

10. Shen A, Wei X, Zhu F, et al. Risk prediction models for breast cancer-related lymphedema: a systematic review and meta-analysis. *Eur J Oncol Nurs*. 2023;64:102326.

11. Gaffney RM, Casley-Smith JR. Excess plasma proteins as a cause of chronic inflammation and lymphoedema: biochemical estimations. *J Pathol*. 1981;133:229–242.

12. Li CY, Kataru RP, Mehrara BJ. Histopathologic features of lymphedema: a molecular review. *Int J Mol Sci*. 2020;21:9–14.

13. Avraham T, Zampell JC, Yan A, et al. Th2 differentiation is necessary for soft tissue fibrosis and lymphatic dysfunction resulting from lymphedema. *FASEB J*. 2013;27:1114–1126.

14. Zampell JC, Elhadad S, Avraham T, et al. Toll-like receptor deficiency worsens inflammation and lymphedema after lymphatic injury. *Am J Physiol Cell Physiol*. 2012;302:C709–C719.

15. Fu MR, Conley YP, Axelrod D, et al. Precision assessment of heterogeneity of lymphedema phenotype, genotypes and risk prediction. *Breast*. 2016;29:231–240.

16. Ryan TJ, De Berker D. The interstitium, the connective tissue environment of the lymphatic, and angiogenesis in human skin. *Clin Dermatol*. 1995;13:451–458.

17. Mihara M, Hara H, Hayashi Y, et al. Pathological steps of cancer-related lymphedema: histological changes in the collecting lymphatic vessels after lymphadenectomy. *PLoS One*. 2012;7:e41126.

18. Kataru RP, Wiser I, Baik JE, et al. Fibrosis and secondary lymphedema: chicken or egg? *Transl Res*. 2019;209:68–76.

19. Will PA, Kilian K, Bieback K, et al. Lymphedema-associated fibroblasts are a TGF-β1 activated myofibroblast subpopulation related to fibrosis and stage progression in patients and a murine microsurgical model. *Plast Reconstr Surg*. 2023. [E-pub ahead of print].

20. Spörlein A, Will PA, Kilian K, et al. Lymphatic tissue engineering: a further step for successful lymphedema treatment. *J Reconstr Microsurg*. 2021;37:465–474.

21. Nakamura K, Radhakrishnan K, Wong YM, et al. Anti-inflammatory pharmacotherapy with ketoprofen ameliorates experimental lymphatic vascular insufficiency in mice. *PLoS One*. 2009;4:e8380.

22. Rockson SG, Tian W, Jiang X, et al. Pilot studies demonstrate the potential benefits of antiinflammatory therapy in human lymphedema. *JCI Insight*. 2018;3:e123775.

23. Azhar SH, Lim HY, Tan BK, et al. The unresolved pathophysiology of lymphedema. *Front Physiol*. 2020;11:137.

24. Hadrian R, Palmes D. Animal models of secondary lymphedema: new approaches in the search for therapeutic options. *Lymphat Res Biol*. 2017;15:2–16.

25. Fischer AH, Jacobson KA, Rose J, et al. Hematoxylin and eosin staining of tissue and cell sections. *CSH Protoc*. 2008;2008:pdb.prot4986.

26. Sweat F, Puchtler H, Rosenthal SI. Sirius red F3BA as a stain for connective tissue. *Arch Pathol*. 1964;78:69–72.

27. Junqueira LC, Bignolas G, Brentani RR. Picrosirius staining plus polarization microscopy, a specific method for collagen detection in tissue sections. *Histochem J*. 1979;11:447–455.

28. Fischer S, Hirche C, Diehm Y, et al. Efficacy and safety of the collagenase of the bacterium Clostridium histolyticum for the treatment of capsular contracture after silicone implants: ex-vivo study on human tissue. *PLoS One*. 2016;11:e0156428.

29. Montes GS, Junqueira LC. The use of the picrosirius-polarization method for the study of the biopathology of collagen. *Mem Inst Oswaldo Cruz*. 1991;86:1–11.

30. Puebla-Osorio N, Sarchio SNE, Ullrich SE, et al. Detection of infiltrating mast cells using a modified toluidine blue staining. *Methods Mol Biol*. 2017;1627:213–222.

31. Maecker HT, McCoy JP, Nussenblatt R. Standardizing immunophenotyping for the human immunology project. *Nat Rev Immunol*. 2012;12:191–200.

32. Schindelin J, Arganda-Carreras I, Frise E, et al. Fiji: an open-source platform for biological-image analysis. *Nat Methods*. 2012;9:676–682.

33. Whittaker P, Kloner RA, Boughner DR, et al. Quantitative assessment of myocardial collagen with picrosirius red staining and circularly polarized light. *Basic Res Cardiol*. 1994;89:397–410.

34. Rich L, Whittaker P. Collagen and picrosirius red staining: a polarized light assessment of fibrillar hue and spatial distribution. *J Morphol Sci*. 2017;22:0–0.

35. Gordon S, Plüddemann A, Martinez Estrada F. Macrophage heterogeneity in tissues: phenotypic diversity and functions. *Immunol Rev*. 2014;262:36–55.

36. Nakai K. Multiple roles of macrophage in skin. *J Dermatol Sci*. 2021;104:2–10.

37. Xue Q, Yan Y, Zhang R, et al. Regulation of iNOS on immune cells and its role in diseases. *Int J Mol Sci*. 2018;19:3805.

38. Murray PJ. Macrophage polarization. *Annu Rev Physiol*. 2017;79:541–566.

39. Parisi L, Gini E, Baci D, et al. Macrophage polarization in chronic inflammatory diseases: killers or builders? *J Immunol Res*. 2018;2018:8917804.

40. Ghanta S, Cuzzone DA, Torrisi JS, et al. Regulation of inflammation and fibrosis by macrophages in lymphedema. *Am J Physiol Heart Circ Physiol*. 2015;308:H1065–H1077.

41. Kataru RP, Jung K, Jang C, et al. Critical role of CD11B+ macrophages and VEGF in inflammatory lymphangiogenesis, antigen clearance, and inflammation resolution. *Blood*. 2009;113:5650–5659.

42. Gardenier JC, Hespe GE, Kataru RP, et al. Diphtheria toxin-mediated ablation of lymphatic endothelial cells results in progressive lymphedema. *JCI Insight*. 2016;1:e84095.

43. Tashiro K, Feng J, Wu SH, et al. Pathological changes of adipose tissue in secondary lymphoedema. *Br J Dermatol*. 2017;177:158–167.

44. Hespe GE, Nores GG, Huang JJ, et al. Pathophysiology of lymphedema—Is there a chance for medication treatment? *J Surg Oncol*. 2017;115:96–98.

45. Drobot A, Bez M, Abu Shakra I, et al. Microsurgery for management of primary and secondary lymphedema. *J Vasc Surg Venous Lymphat Disord*. 2021;9:226–233.e1.

46. Chang DW, Suami H, Skoracki R. A prospective analysis of 100 consecutive lymphovenous bypass cases for treatment of extremity lymphedema. *Plast Reconstr Surg*. 2013;132:1305–1314.

47. Schaverien MV, Coroneos CJ. Surgical treatment of lymphedema. *Plast Reconstr Surg*. 2019;144:738–758.

48. Will PA, Hirche C, Berner JE, et al. Lymphovenous anastomoses with three-dimensional digital hybrid visualization: improving ergonomics for supermicrosurgery in lymphedema. *Arch Plast Surg*. 2021;48:427–432.

49. Zampell JC, Aschen S, Weitman ES, et al. Regulation of adipogenesis by lymphatic fluid stasis part I: adipogenesis, fibrosis, and inflammation. *Plast Reconstr Surg*. 2012;129:825–834.

50. von Atzigen J, Burger A, Grünherz L, et al. A comparative analysis to dissect the histological and molecular differences among lipedema, lipohypertrophy and secondary lymphedema. *Int J Mol Sci*. 2023;24:7591.

51. Wolf S, von Atzigen J, Kaiser B, et al. Is lymphedema a systemic disease? a paired molecular and histological analysis of the affected and unaffected tissue in lymphedema patients. *Biomolecules*. 2022;12:1667.

52. Will P, Rafiei A, Pretze M, et al. Evidence of stage progression in a novel, validated fluorescence-navigated and microsurgical-assisted secondary lymphedema rodent model. *PLoS One*. 2020;15:e0235965.

53. Di S, Ziyou Y, Liu NF. Pathological changes of lymphedematous skin: increased mast cells, related proteases, and activated transforming growth factor-beta1. *Lymphat Res Biol*. 2016;14:162–171.

54. Kimura T, Sugaya M, Blauvelt A, et al. Delayed wound healing due to increased interleukin-10 expression in mice with lymphatic dysfunction. *J Leukoc Biol*. 2013;94:137–145.

55. Kunder CA, St John AL, Abraham SN. Mast cell modulation of the vascular and lymphatic endothelium. *Blood*. 2011;118:5383–5393.

56. Plaku KJ, von der Weid PY. Mast cell degranulation alters lymphatic contractile activity through action of histamine. *Microcirculation*. 2006;13:219–227.

57. Schirger A. Postoperative lymphedema: etiologic and diagnostic factors. *Med Clin North Am*. 1962;46:1045–1050.

58. Karayi AK, Basavaraj V, Narahari SR, et al. Human skin fibrosis: up-regulation of collagen type III gene transcription in the fibrotic skin nodules of lower limb lymphoedema. *Trop Med Int Health*. 2020;25:319–327.

59. Tassenoy A, De Mey J, Stadnik T, et al. Histological findings compared with magnetic resonance and ultrasonographic imaging in irreversible postmastectomy lymphedema: a case study. *Lymphat Res Biol*. 2009;7:145–151.

60. Rutkowski JM, Moya M, Johannes J, et al. Secondary lymphedema in the mouse tail: Lymphatic hyperplasia, VEGF-C upregulation, and the protective role of MMP-9. *Microvasc Res*. 2006;72:161–171.

61. Rutkowski JM, Markhus CE, Gyenge CC, et al. Dermal collagen and lipid deposition correlate with tissue swelling and hydraulic conductivity in murine primary lymphedema. *Am J Pathol*. 2010;176:1122–1129.

62. Morfoisse F, Zamora A, Marchaud E, et al. Sex hormones in lymphedema. *Cancers (Basel)*. 2021;13:530.

63. Will PA, Wan Z, Seide SE, et al. Supermicrosurgical treatment for lymphedema: a systematic review and network meta-analysis protocol. *Syst Rev*. 2022;11:18.

64. Diehm YF, Thomé J, Will P, et al. Stem-cell enriched hybrid breast reconstruction reduces risk for capsular contracture in a hybrid breast reconstruction animal model. *Plast Reconstr Surg*. 2023;152:572–580.

65. Kølle SF, Fischer-Nielsen A, Mathiasen AB, et al. Enrichment of autologous fat grafts with ex-vivo expanded adipose tissue-derived stem cells for graft survival: a randomised placebo-controlled trial. *Lancet*. 2013;382:1113–1120.

66. Scaglioni MF, Arvanitakis M, Chen YC, et al. Comprehensive review of vascularized lymph node transfers for lymphedema: outcomes and complications. *Microsurgery*. 2018;38:222–229.

67. Bernas MJ, Askew RL, Armer JM, et al. Lymphedema: how do we diagnose and reduce the risk of this dreaded complication of breast cancer treatment? *Curr Breast Cancer Rep*. 2010;2: 53–58.